Al-Kitab Journal for Pure Sciences (2026); 10(1):243-263.
https://doi.org/10.32441/kjps.10.1.p15

Al-Kitab Journal for Pure Sciences
ISSN: 2617-1260 (print), 2617-8141(online)

https://isnra.net/index.php/kjps

Synthesis of Triazole-Imine Derivatives with Antibacterial and Anticancer Potential: An Experimental and in Silico Study

Diaa M. Najim

Kirkuk Education Directorate

Corresponding Auther: info@researchcenter.iq

Citation: ***Diaa M. Najim.*** **Synthesis of Triazole-Imine Derivatives with Antibacterial and Anticancer Potential: An Experimental and in Silico Study.** Al-Kitab J. Pure Sci. [Internet]. 2026 Mar. 07; 10(1):243-263 DOI:

https://doi.org/10.32441/kjps.10.1.p15

Keywords: Molecular docking, Schiff bases, Triazole derivatives, Heterocyclic compounds.

.

Article History

Received	20 Jan. 2026
Accepted	07 Mar. 2026
Available online	01 May. 2026

Abstract:

This work condensed 4-hydroxybenzaldehyde and triazole-based primary amines to form triazole–imine compounds (A–D). Generated compounds revealed azomethine links in FTIR and NMR. *Streptococcus pneumoniae* and *Bacillus subtilis* antibacterial activity was measured by 0.1, 0.001, and 0.00001 mg/mL agar diffusion derivative C had the largest concentration-dependent inhibition zones of 23 mm against *S. pneumoniae* and 25 mm against *B. subtilis*. MTT also assessed PC-3 and MCF-7 cytotoxicity. The derivative A dose-dependently reduced PC-3 and MCF-7 cell viability by 4.99% and 8%, respectively, at 320 µg/mL. Docking DNA-associated protein (8RZX) explains these biological results. Docking data show stable binding conformations, with RMSD values around 2 Å and binding energies −2.5 kcal/mol, especially for derivative C. The majority of interactions were hydrogen bonding with phosphate groups and π–π stacking with nucleobases. Experimental and computational evidence suggest triazole–imine compounds are potential antibacterial and anticancer scaffolds.

Keywords: Molecular docking, Schiff bases, Triazole derivatives, Heterocyclic compounds.

تحضيرمشتقات التريازول- إيمين كعوامل واعدة مضادة للبكتيريا والسرطان: دراسة تجريبية وحاسوبية

ضياء محمود نجم

diaa1988mahmoud@gmail.com

الخلاصة:

في هذه الدراسة، تم تكثيف ٤-هيدروكسي بنزالدهيد مع الأمينات الأولية القائمة على التريازول لتكوين مركبات تريازول-إيمين (*A-D*). اظهر طيف الاشعة تحت الحمراءوطيف الرنين النووي المغناطيسي عن وجود روابط أزوميثين في المركبات المُنتجة. تم قياس النشاط المضاد للبكتيريا ضد المكورات الرئوية (*Streptococcus pneumoniae*) والعصوية الرقيقة (*Bacillus subtilis*) باستخدام تراكيز ٠,١ و٠,٠٠١ و٠,٠٠٠٠١ ملغم/مل من مشتق الأجار *C*، حيث أظهر أكبر مناطق تثبيط معتمدة على التركيز، بقطر ٢٣ مم ضد المكورات الرئوية و٢٥ مم ضد العصوية الرقيقة. كما تم تقييم سمية المركبين *PC-3* و*MCF-7* باستخدام اختبار *MTT*. أدى المشتق *A* إلى خفض حيوية خلايا *PC-3* و*MCF-7* بنسبة ٤,٩٩٪ و٨٪ على التوالي، عند تركيز ٣٢٠ ميكروغرام/مل، وذلك بشكل متناسب مع الجرعة. ويُفسر ارتباط البروتين المرتبط بالحمض النووي (*RZX٨*) هذه النتائج البيولوجية. تُظهر بيانات الارتباط تكوينات ارتباط مستقرة، بقيم *RMSD* تقارب ٢ أنغستروم وطاقات ارتباط تبلغ -٢,٥ كيلو كالوري/مول، وخاصةً بالنسبة للمشتق *C*. وكانت غالبية التفاعلات عبارة عن روابط هيدروجينية مع مجموعات الفوسفات وتفاعلات تكديس *π-π* مع القواعد النيتروجينية. تشير الأدلة التجريبية والحسابية إلى أن مركبات التريازول-إيمين تُعدّ هياكل محتملة مضادة للبكتيريا ومضادة للسرطان.

الكلمات المفتاحية: الالتحام الجزيئي، قواعد شيف، مشتقات التريازول، المركبات الحلقية غير المتجانسة.

1. Introduction:

Heterocyclic compounds play a crucial role in medicinal chemistry due to their diverse biological activities [1]. Synthesis of heterocyclic chemical compounds is an important priority in organic chemical synthesis due to its many uses in health, pharmacology, electronic devices, agricultural production, and other associated domains [2].Two essential requirements must be addressed by contemporary heterocyclic chemistry methods (reagents, techniques, strategies, reaction processes, chemical and instrumental auxiliaries, catalysts, etc.): "specificity" and "selectivity" (containing common prefixes like chemo, regio, or stereo) [3]. There are two isomers of the triazole ring, a notable five-membered heterocycle containing three nitrogen atoms: The aromatic system 1,2,3-triazole, also known as 1,2,4-triazole, is rich in electrons. Through weak interactions like coordination bonds, hydrogen bonds, ion-dipole interactions, cation stacking, hydrophobic effect, van der Waals force, and so forth. This kind of special

structure enables triazole derivatives to readily bind with a variety of enzymes and receptors in biological systems, leading to a wide range of biological activities[4-6].

Schiff bases, or imines, are essential organic structural motifs. Reversible condensation reactions between a carbonyl molecule and a primary amine generate imines, which have a carbon–nitrogen double bond. Drying agents, molecular sieves, or Dean–Stark traps remove water from the process [7]. Imines are valuable as catalytic ligands, intermediates in the synthesis of nitrogen-containing heterocycles and alkaloids, and players in coordination chemistry. Dantrolene, a muscle relaxant, and thiacetazone, an antituberculosis medication, contain imines [8]. Several organic laboratories have imine synthesis reactions, despite their abundance in biochemical processes in nature. In light of this, a lab study involving imine-based chemical synthesis is crucial[9].

Recent research has focused on triazole-associated Schiff bases with different substituents for antibacterial and anticancer properties. Few studies have linked spectroscopic confirmation, in vitro biological evaluation, and in silico docking against DNA-linked target proteins like PDB ID: 8RZX. Thus, there is little experimental and molecular study on how triazole-imine framework structural variation impacts binding affinity, antibacterial activity, and cytotoxicity.

New triazole-imine molecules are synthesized and tested for biological activity using complementary approaches. The primary research questions: How do triazole amine precursors affect Schiff bases' physicochemical and biological properties? Working with the 8RZX binding pocket, molecular docking may explain antibacterial and anticancer action differences. Answering these questions requires several steps. FTIR and NMR the target derivative structure following synthesis. Their antibacterial and cytotoxic properties against Gram-positive bacteria and PC-3 and MCF-7 cancer cells are tested. Finally, molecular docking examines binding modes, interaction energies, and structure–activity relationships. Triazole–imine molecules are intriguing bioactive candidates, and this work applies this integrated approach.

2.Material and methods:

2.1 Material.

Sigma Aldrich provided a variety of amines, including 4-Amino-1,2,4-triazole, 3-Amino-1,2,4-triazole, 3-Amino-5-methylthio-1H-1,2,4-triazole, and 5-Amino-1H-[1,2,4]-triazole-3-carboxylic acid methyl ester. While 100% ethanol, glacial acetic acid, and 4-hydroxybenzaldehyde were acquired from BDH.

2.2 Synthesis of schiff base derivatives (A-D).

According to Jaafar, M. R., et al (2024) [10], a novel group of imine derivatives (A-D) was synthesized by reacting the same moles of 4-hydroxybenzaldehyde with varying derivatives of triazole that were classified as primary amines. 0.1 mole of 4-hydroxy benzaldehyde dissolved in 20 mL of absolute ethanol, and add 2-3 drops of glacial acetic acid; add the amine compound to this solution, and reflux for 3 hours. The mixture is then cooled to room temperature and filtered to collect the precipitate. To synthesize derivative A obtained from 4-amino-1,2,4-triazole; derivative B from 3-Amino-1,2,4-triazole; derivative C from 3-Amino-5-methylthio-1H-1,2,4-triazole; derivative D from 5-Amino-1H-[1,2,4]-triazole-3-carboxylic acid methyl ester, as shown in **Scheme 1**.

The physical properties of synthesized derivative A were obtained as a dark yellow precipitate and have melting point (١٨٧°C). In contrast, derivative B was obtained as a yellow color and (161°C) with a melting point, and derivative C was yellowish-brown had a melting of (143°C). Finally, derivative D was formed in a dark yellow and 181°C.

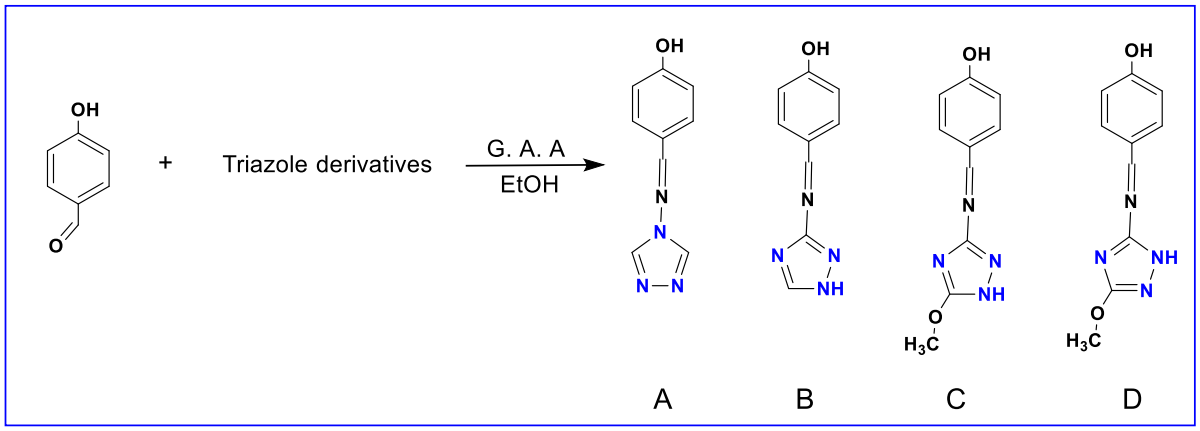

Scheme 1: Synthesized triazole-imine derivatives (A-D).

2.3 Assessment of Antimicrobial Properties of Schiff bases Derivatives.

The cup-plate agar diffusion technique evaluates the antibacterial efficacy of derivatives A-C. *Streptococcus pneumoniae* and *Bacillus subtilis* isolated from clinical infections are designated as test organisms. Compounds are formulated in dimethyl sulfoxide at three concentrations: 0.1, 0.001, and 0.00001 mg/mL. Muller-Hinton agar plates are inoculated with bacterial suspensions, and 12 mm wells are filled with the test solutions. Ceftriaxone reconstituted in sterile water serves as the reference standard. Following one hour of pre-diffusion, the plates were incubated..." (add what happens next). The antibacterial efficacy of each chemical is evaluated by measuring the inhibition zone diameter in millimeters and comparing it to the reference medicine **[11].**

2.4 The Biotech MTT kit was used to assess several synthetic compounds for cytotoxicity.

Synthesized molecules were evaluated for cytotoxicity against prostate cancer PC3 cells with the MTT assay according to the manufacturer's instructions. MCF-7 cells were seeded at 4.5 × 10^5 per well in sterile 96-well plates containing 200 µL of growth medium. To improve cell adherence, plates were sealed with parafilm, lightly centrifuged, and incubated at 37 °C in 5% CO_2 for 24 hrs. Cells were subjected to a 2-fold serial dilution and treated with synthetic derivatives at concentrations of 0, 20, 40, 80, 160, and 320 µg/mL after incubation. The controlled plate was incubated for 24 hours. Following drug exposure, each well received 10 µL of MTT solution, which was then incubated for 4 hours to allow metabolically active cells to transform MTT into insoluble formazan crystals. After incubation, remove the supernatant and dissolve the formazan in 100 µL of DMSO in each well to preserve the crystals. After five minutes of moderate swirling, the plates melted. 575 nm absorbance was measured using ELISA microplate readers (Bio-Rad, Germany). Cell viability was shown by optical density measurements, and the half-maximal inhibitory concentration (IC_{50}) of the derivatives was ascertained using statistical analysis. This technique assessed cytotoxic effects accurately, consistently, and dependably **[12]**.

2.5 Molecular Docking Process

To investigate the binding mechanism and affinity, the chemically generated triazole–imine compounds (A–C) were docked with the biological target protein (PDB ID: 8RZX) using the Molecular Operating Environment (MOE) tool **[13, 14]. Figure 1**. Its three-dimensional crystal structure was taken from the Protein Data Bank and generated in MOE by removing crystallographic water molecules and co-crystallized ligands to reduce ligand binding interference. We inserted hydrogen atoms and energy-minimized the protein structure to decrease steric conflicts and maximize form **[15]**. MOE imported ligand chemical structures drawn in Chem Draw. Ligands were translated into three-dimensional conformations and geometry was adjusted using a force field to create stable structures. For docking, partial atomic charges and rotatable bonds were assigned for conformational flexibility **[16]**. The MOE docking simulation active binding area was defined by 8RZX binding pocket nucleotide residues. The placement strategy produced various active site ligand postures. A scoring function calculated the binding free energy. After energy reduction improved top-ranked postures, docking scores, interaction types, and RMSD values were gathered. The research

studied ligand-protein interactions, including hydrogen bonding, π-π stacking, and binding distances.

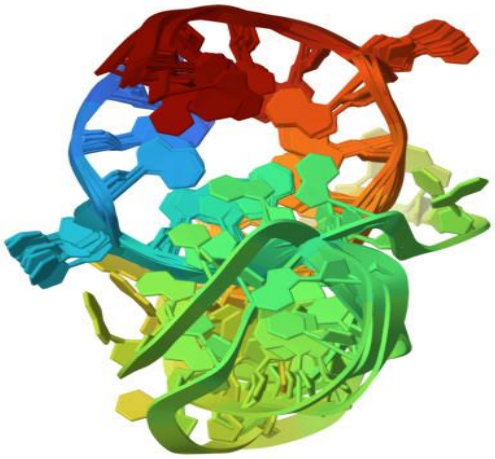

Figure 1: Chemical structure of 8RZX protein.

3.Results and Discussion

The reaction between 4-hydroxybenzaldehyde and different primary amines to produce Schiff base derivatives results in different yellow colors as precipitates. In these reactions, the glacial acetic acid plays a catalytic role to protonate the carbonyl group, and the amine derivative plays a nucleophilic role to attack the carbon of the carbonyl group. In FTIR spectroscopy, the primary amine and the carbonyl group of the aldehyde disappeared and showed a new peak for the imine group **[17, 18]**.

4-(((4H-1,2,4-triazol-4-yl)imino)methyl)phenol (A).

The FTIR (cm^{-1}) spectrum shows a peak at 1625 for azo methane group **[19]**, 3336 for the hydroxyl group as broad band, 3029 for the C-H of the aromatic ring, and 1580 for C=C of aromatic ring. ^{1}H-NMR (DMSO-d6 as solvent) δ 9.15 (s, 1H, -OH), 8.49 (s, 1H, imine), 7.71 – 7.18 (m, 4H , Ar), as shown in **Figure 2**. ^{13}C-NMR (DMSO-d_6) the key peaks include 155.33 ppm (C-OH), 149.65 ppm (triazole carbon), and 138.87 ppm (ipso-carbon bonded to the linkage). Aromatic methine carbons (CH) appeared at 133.16 and 125.71 ppm, while the ortho-carbons shifted upfield to 114.56 ppm due to the electron-donating effect of the hydroxyl group **[20]**, as shown in **Figure 3.**

4-(((1H-1,2,4-triazol-3-yl)imino)methyl)phenol (B).

The FTIR (cm^{-1}) spectrum shows a peak at 1641 for imine group, 3335 for the hydroxyl group, 3055 for the C-H of the aromatic ring and 1582 for C=C of aromatic ring **[21]**. ^{1}H NMR

(DMSO-d_6) δ 9.91 (s, 1H, -OH), 8.98 (s, 1H, imine), 8.15-7.24 (m, 5H, Ar), as shown in **Figure 4**. ^{13}C NMR (DMSO-d_6) δ 161.01 for aromatic carbon that linked to hydroxyl group, 153.76 for carbon imine group, 149.50-113.81 for aromatic carbon **[22]**, as shown in **Figure 5**.

4-(((5-methoxy-1H-1,2,4-triazol-3-yl)imino)methyl)phenol (C).

The FTIR (cm^{-1}) spectrum shows a peak at 1631 for imine group, 3384 for the secondary amine, 3025 for the C-H of the aromatic ring and 1579 for C=C of aromatic ring **[21]**.^{1}H-NMR (DMSO-d_6) δ 9.09 (s, 1H, -OH), 8.67 (s, 1H, imine), 7.75-7.24 (m, 4H, Ar), 5.29 (s, 1H, NH), 3.89 (s, 3H, methoxy)**[11]**, as shown in **Figure 6**. ^{13}C-NMR (50 MHz, DMSO-d_6) δ 162.81 for aromatic carbon that linked to hydroxyl group, 157.70 for carbon triazine ring that linked to oxygen of methoxy group, 152.97 for carbon imine group, 148.02-108.61 for aromatic carbon, 61.26 for methoxy group **[23]**, as shown in **Figure 7**.

4-(((3-methoxy-1H-1,2,4-triazol-5-yl)imino)methyl)phenol (D).

The FTIR (cm^{-1}) spectrum shows a peak at 1621 for imine group, 3363 for the secondary amine, 3068 for the C-H of the aromatic ring and 1598 for C=C of aromatic ring.^{1}H NMR (DMSO-d_6) δ 9.01 (s, 1H, -OH), 8.11,(s, 1H, imine), 7.64-7.01 (m, 4H, Ar), 5.26 (s, 1H, NH) **[24]**, 2.98 (s, 3H, methoxy) [10], as shown in **Figure 8**. ^{13}C NMR (DMSO-d_6) δ 162.52 carbon of imine group, 155.49 for carbon triazine ring that linked to oxygen of methoxy group,155.27 aromatic carbon that linked to hydroxyl group, 154.07-122.95 carbons of aromatic group, 59.92 carbon of methoxy group **[25]**, as shown in **Figure 9.**

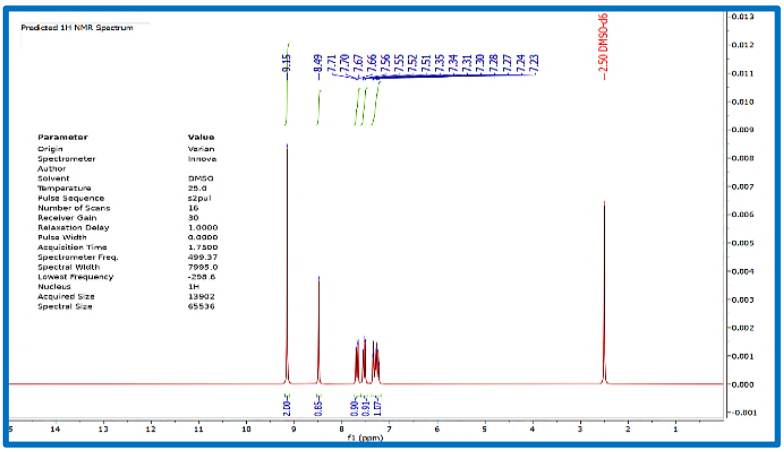

Figure 2: ^{1}H-NMR spectrum of derivative A.

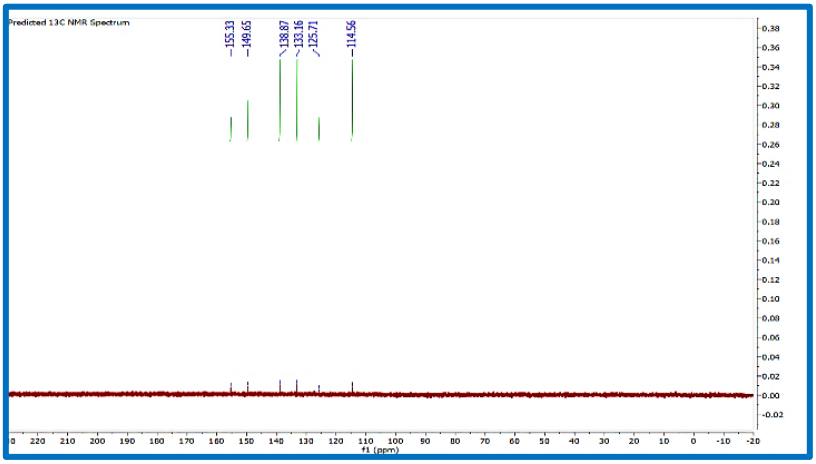

Figure 3: ^{13}C-NMR spectrum of derivative A.

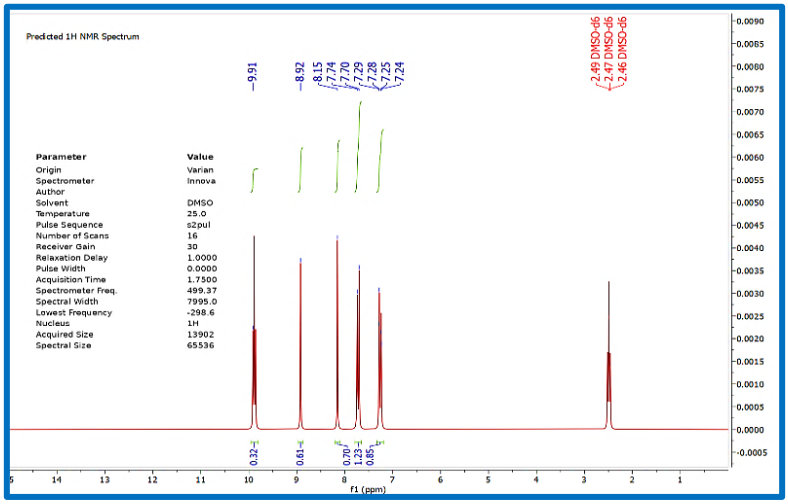

Figure 4: ^{1}H-NMR spectrum of derivative B.

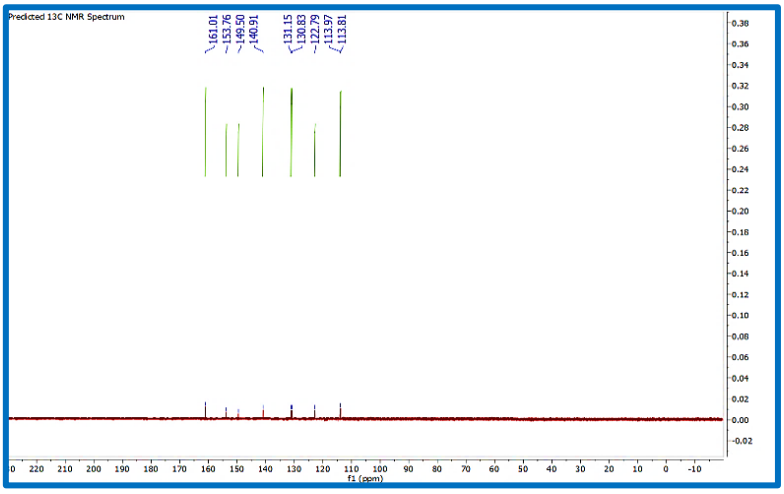

Figure 5: ^{13}C-NMR spectrum of derivative B.

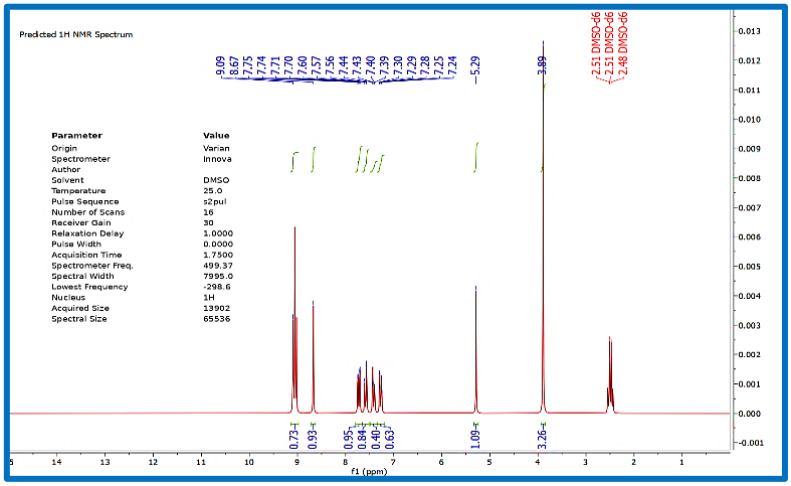

Figure 6: ^{1}H-NMR spectrum of derivative C.

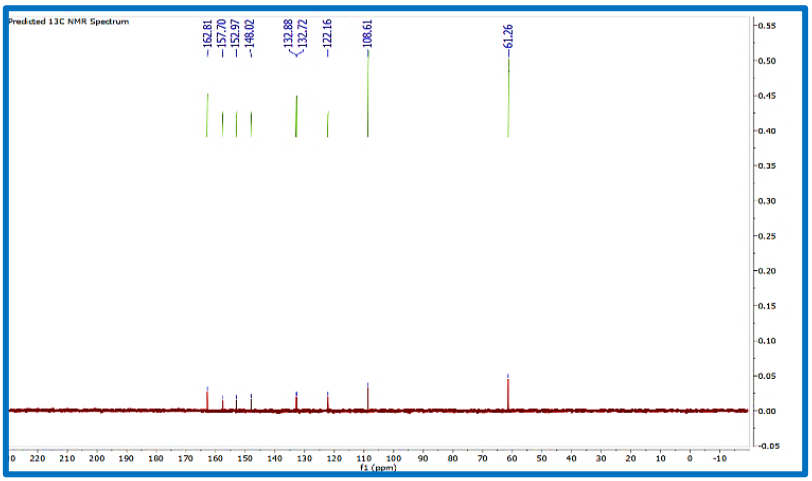

Figure 7: ^{13}C-NMR spectrum of derivative C.

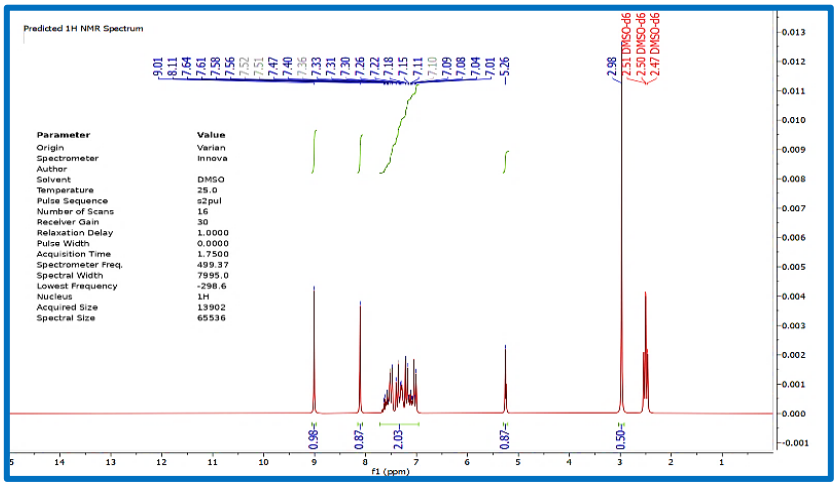

Figure 8: ^{1}H-NMR spectrum of derivative D.

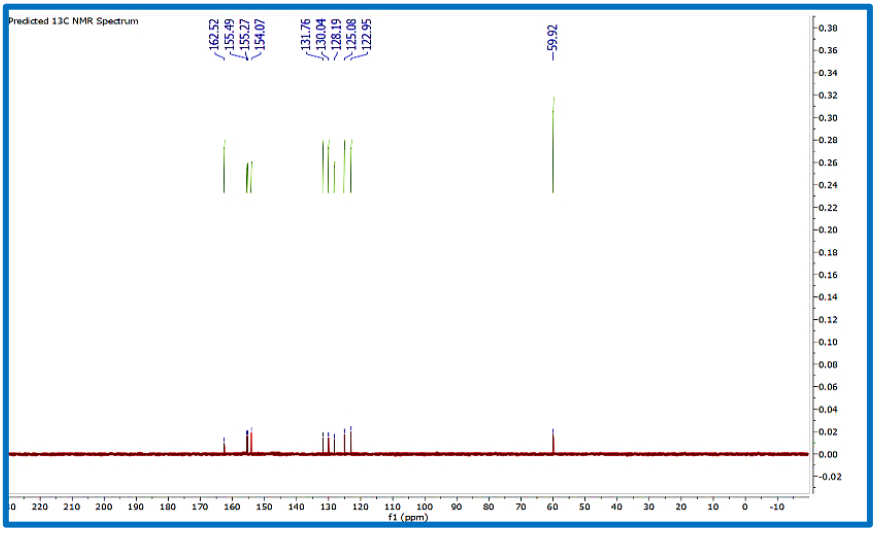

Figure 9: ^{13}C-NMR spectrum of derivative D.

The 8RZX protein has a well-defined binding pocket composed of DNA nucleotides such as DT, DC, DA, and DG. The pocket's mild polarity and aromaticity facilitate the stability of organic ligands by hydrogen bonding with phosphate groups and π–π stacking with nucleobases. The structural characteristics render 8RZX suitable for bioactive ligand evaluation by molecular docking **[26].**

Table 1 describes the physicochemical parameters of the active site of the 8RZX protein. The moderate size of the binding pocket accommodates small aromatic ligands without steric hindrance. Numerous nucleotide residues, particularly DG and DT units, provide a hybrid polar and aromatic milieu. Heteroatom as an aromatic ring ligands bind strongly because of these characteristics, selective and stable ligand binding and docking interactions of synthetic molecules are made possible by the pocket structure.

Table 1: Binding Pocket Characteristics of 8RZX Protein.

Site	Size	PLB	Hyd	Side	Residues
1	50	2.4	7	51	1:(DT1 DC12 DA13 DG14 DG15 DT16 DG17 DG18 DG19 DC20 DG21)

The synthetic 8RZX protein with synthesized derivatives (A-C) together with their docking contacts and binding energies are listed in **Table 2**. The hydrogen bonds that Compound A forms with DG21's OP1 show polar anchoring of the binding site. Compound B's π–π stacking and hydrogen bonding with DG19 and DG21 show enhanced stability via dual contact

mechanisms. The most intricate interactions are shown by compound C, which forms π–π stacking with DG21 and hydrogen bonds with DG19. Ligand-protein stability is indicated by moderate binding energies and contact distances. Heteroatoms and aromatic systems boost binding affinity, but compound C exhibits superior active site spatial complementarily compared to the others.

Table 2: Docking results for synthesized derivatives interaction with target protein.

Compound No.	Ligand	Receptor	Interaction	Distance (Å)	E (kcal/mol)
A	O 11	OP1 DG 21 (A)	H-donor	3.16	-2.5
B	O 11	OP1 DG 19 (A)	H-donor	2.97	-2.5
	5-ring	5-ring DG 21 (A)	π–π	3.96	
C	O 15	OP1 DG 19 (A)	H-donor	2.92	-2.1
	5-ring	5-ring DG 21 (A)	π–π	3.71	
	5-ring	6-ring DG 21 (A)	π–π	3.60	

Table 3 displays the medicines' energy components, RMSD values, and 8RZX receptor docking scores. With RMSD values close to 2 Å, all compounds show stable binding orientations. Compound C has the best docking, indicating stability throughout placement and refinement. Compounds A and B score well after docking and refining. Favorable intermolecular interactions that encourage spontaneous ligand-protein attachment are indicated by negative binding scores. Hydrogen bonding and π–π stacking in compounds are impacted by changes in functional groups and aromatic substitution. Research indicates that modifications to the ligand scaffold significantly influence binding at the 8RZX active site.

Table 3: Interaction details of the synthesized derivatives and the protein acceptor.

Compound No.	Image
A	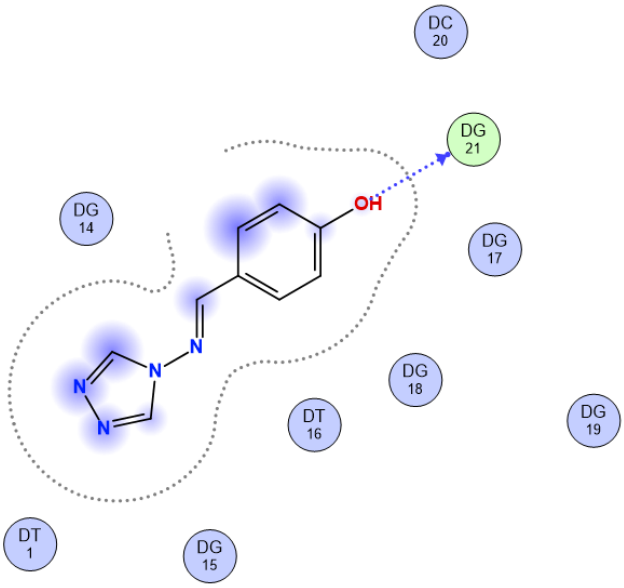
B	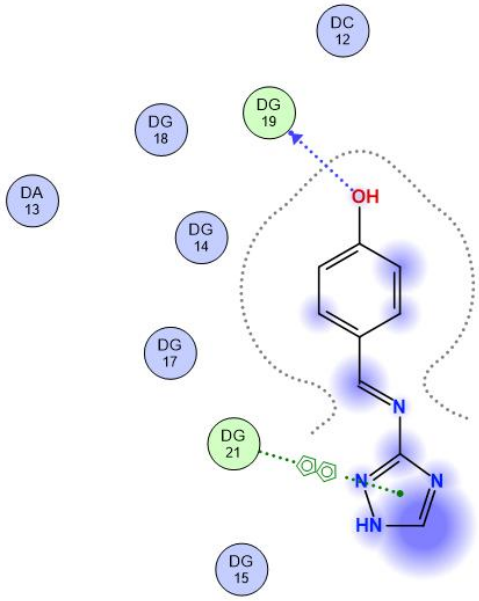

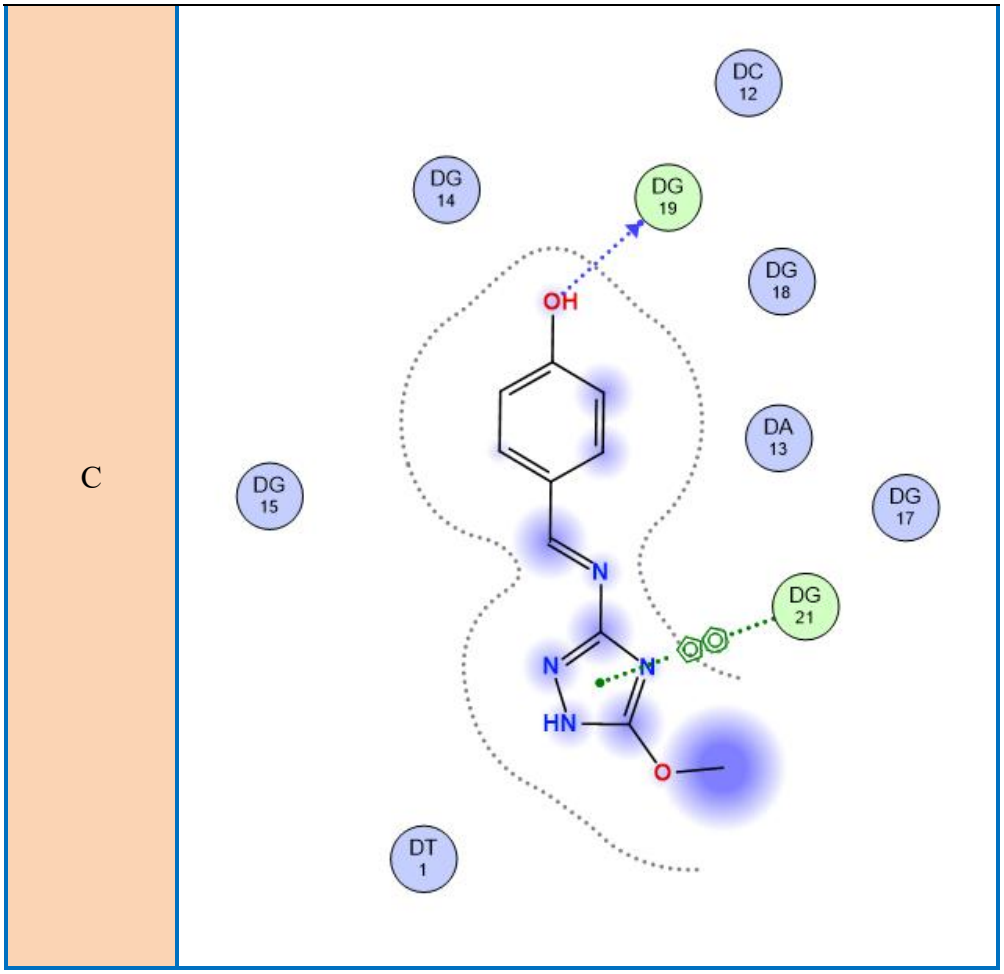

Each of the derivatives inhibits *Streptococcus pneumoniae* in a dose-dependent manner. At the highest concentration, compound C (23 mm) has the greatest activity among the synthesized derivatives, followed by derivative D (20 mm), derivative B (17 mm), and A (15 mm). The optimal standard is 25 mm azithromycin. The inhibitory zones of derivative A significantly decrease at middle and low dosages, indicating less activity persistence. The derivative C is the most promising derivative against S. pneumonia, demonstrating sustained suppression comparable to the reference antibiotic at elevated doses, as shown in **Figure 10.**

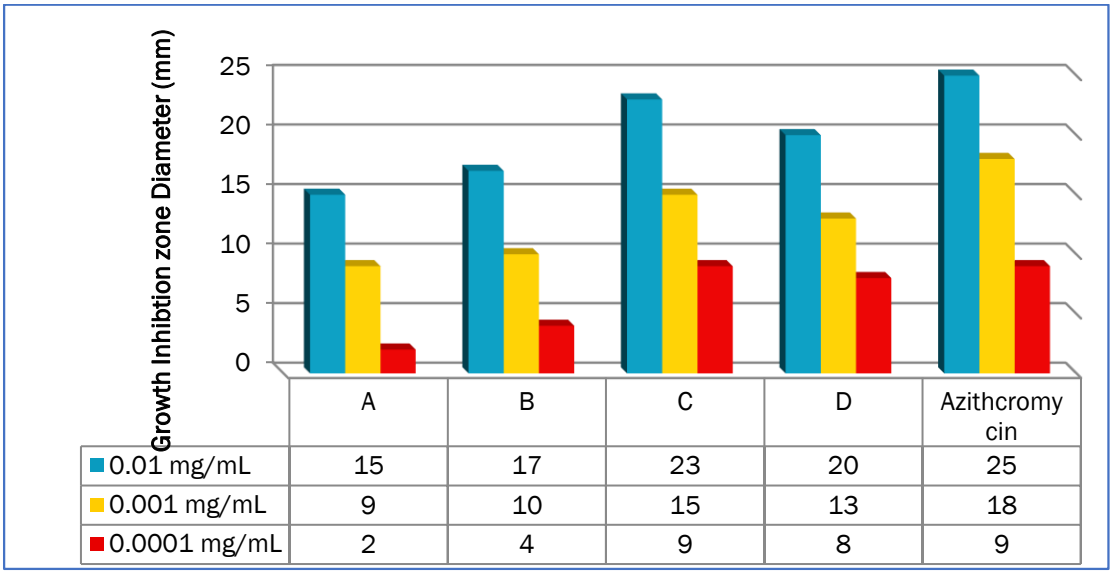

Figure 10: Synthesized derivatives activity of against *Streptococcus pneumonia*.

Each synthesized derivative has concentration-dependent *Bacillus subtilis* antibacterial activity. At 0.1 dosage, derivative C (25 mm) and derivative D (23 mm) had the largest inhibitory zones, reaching azithromycin (24 mm). Both derivative A (18 mm) and derivative B (16 mm) demonstrated modest action at equal doses. At concentrations of 0.001 and 0.00001, inhibition zones markedly decrease for all derivatives, indicating reduced efficacy at lower doses. Derivatives C and D exhibit superior antibacterial efficacy compared to derivative A and derivative B, suggesting enhanced interaction with bacterial targets, as shown in **Figure 11.**

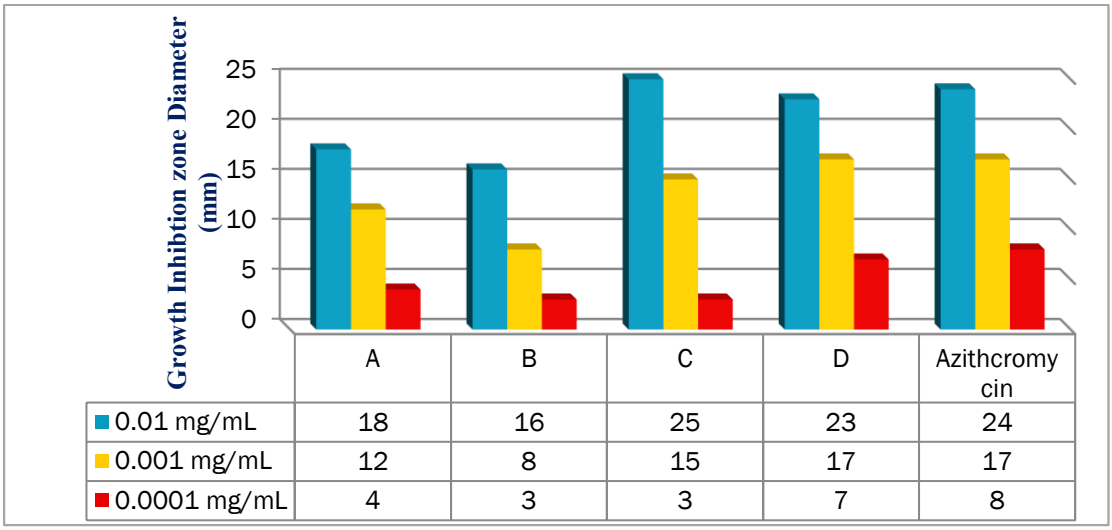

Figure 11: Antibacterial activity of synthesized derivatives against *Bacillus subtilis*.

This figure demonstrates A's concentration-dependent cytotoxicity against PC-3 cells. Cell viability decreases from 99.69% in the control group to 59.26% and 44.51% at 20 and 40 ppm. At the maximum dosage, viability is reduced to 4.99% by high dosages (80–320 ppm). This notable decline seems to have the potential to impede development and cause cell death.

Because of its consistent trend throughout concentrations, chemical A may combat prostate cancer at high doses, as shown in **Figures 12 and 13.**

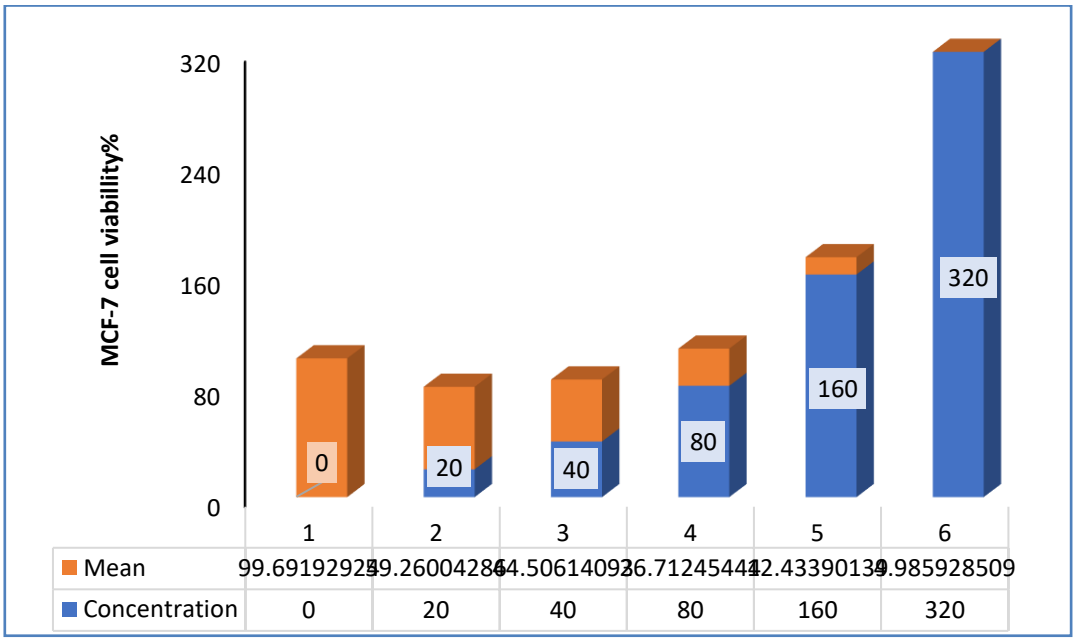

Figure 12: Cytotoxicity of MCF-7 Cells to increasing concentrations of derivative A.

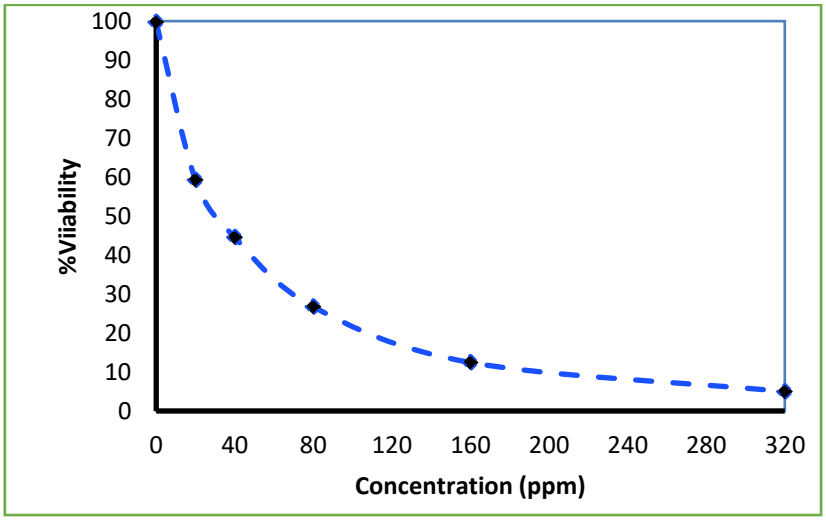

Figure 13: Dose response curve illustrating the cytotoxic effect of derivative A on MCF-7 Cells.

Concentration-dependent Compound C cytotoxicity against MCF-7 cells. Control group cell viability remains almost unaltered, indicating normal cell growth. Growth inhibition is seen between 20 and 40 ppm, when viability reduces to 61% and 50%. Higher dosages reduce viability to 33.5% at 80 ppm and 8% at 320 ppm. This slow fall reveals that derivative C restricts cell proliferation and may kill cells at high doses. The derivative C has exceptional antitumor potential against MCF-7 cells, as shown in **Figures 14 and 15**.

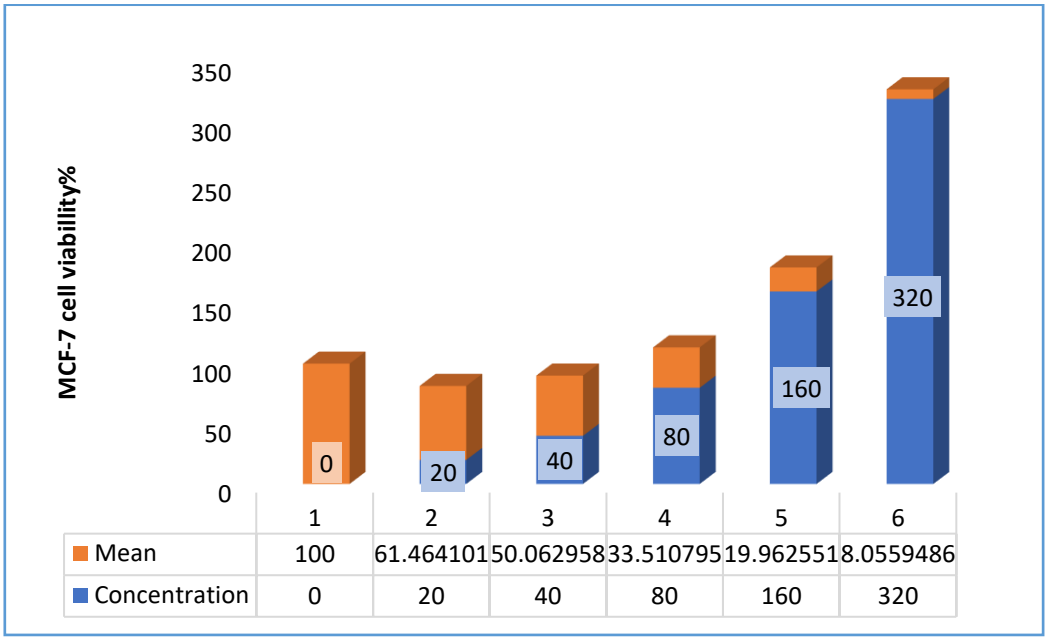

Figure 14: Cytotoxicity of MCF-7 Cells to increasing concentrations of derivative C.

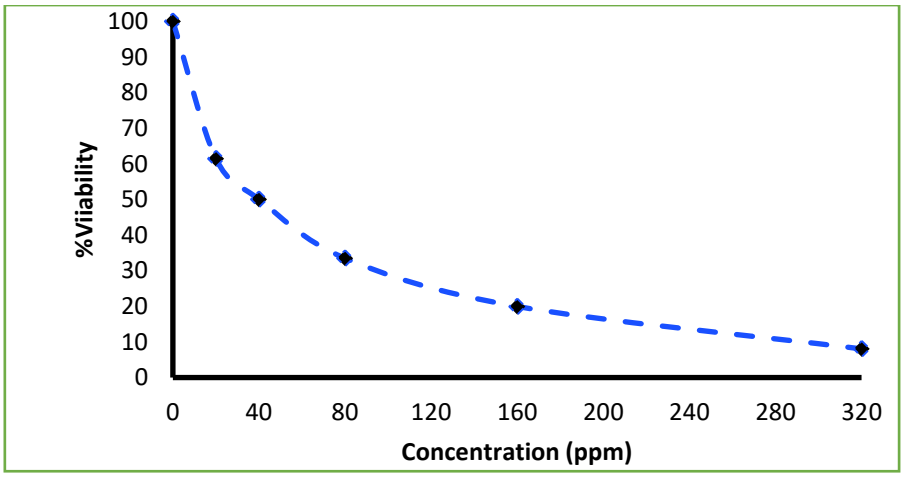

Figure 15: Dose response curve illustrating the cytotoxic effect of derivative C on MCF-7 Cells.

The predicted ADMET profiles for derivatives A-D (**Figures 16-19**) show drug-likeness and pharmacokinetics. All derivatives have molecular weights below 250 g/mol and pass Lipinski's rule of five without exception, indicating oral drug-like characteristics. The consensus LogP values of 1.1–1.8 imply balanced lipophilicity, which improves membrane permeability and water solubility. All compounds are predicted to be water-soluble, which aids formulation and absorption. Pharmacokinetic estimates imply oral uptake due to high gastrointestinal absorption for all derivatives. Anticancer and antibacterial compounds are unlikely to cross the blood-brain barrier, reducing central nervous system side effects. Without P-glycoprotein substrate behavior, efflux-mediated drug resistance is unlikely. Importantly, the compounds do not

inhibit critical cytochrome P450 enzymes, indicating low metabolic drug-drug interactions. The absence of PAINS alerts in medicinal chemistry improves confidence in experimental data's biological relevance, whereas the imine functionality Brenk alarm is expected and chemically justified. ADMET analysis confirms experimental findings and reveals that produced triazole-imine compounds have appropriate pharmacokinetic properties for optimization and biological evaluation.

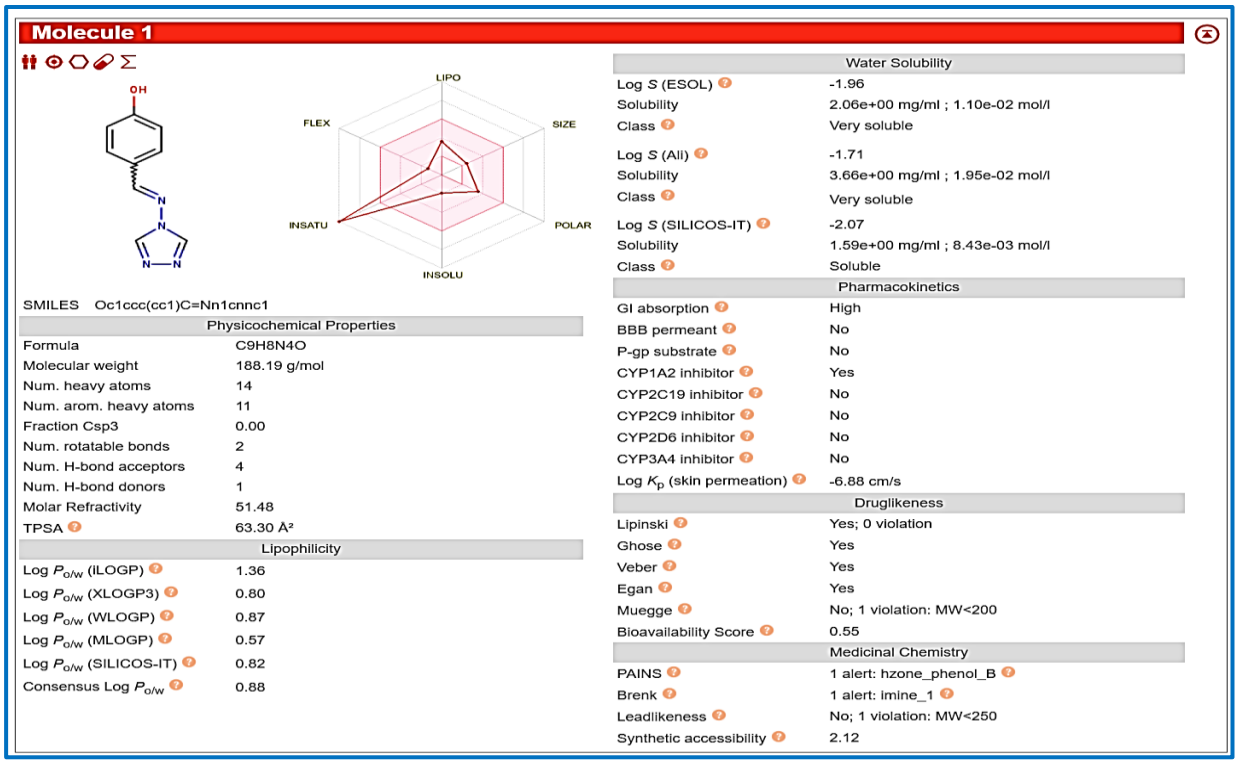

Figure 16: SwissADME Prediction for derivative A.

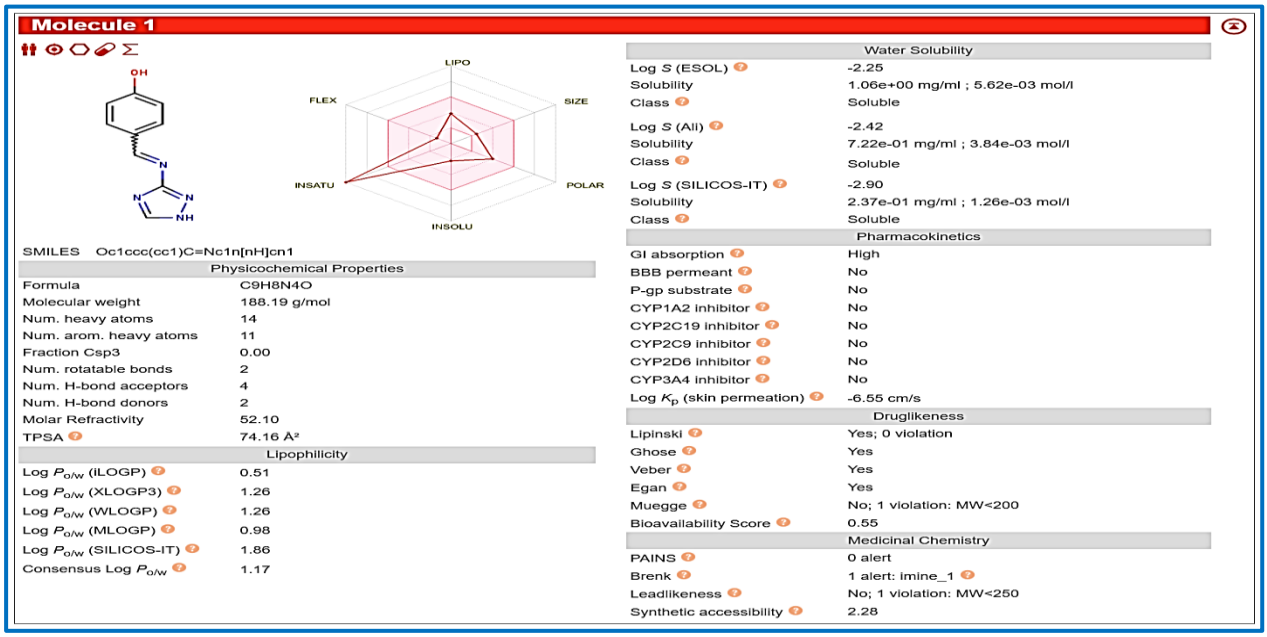

Figure 17: SwissADME Prediction for derivative B.

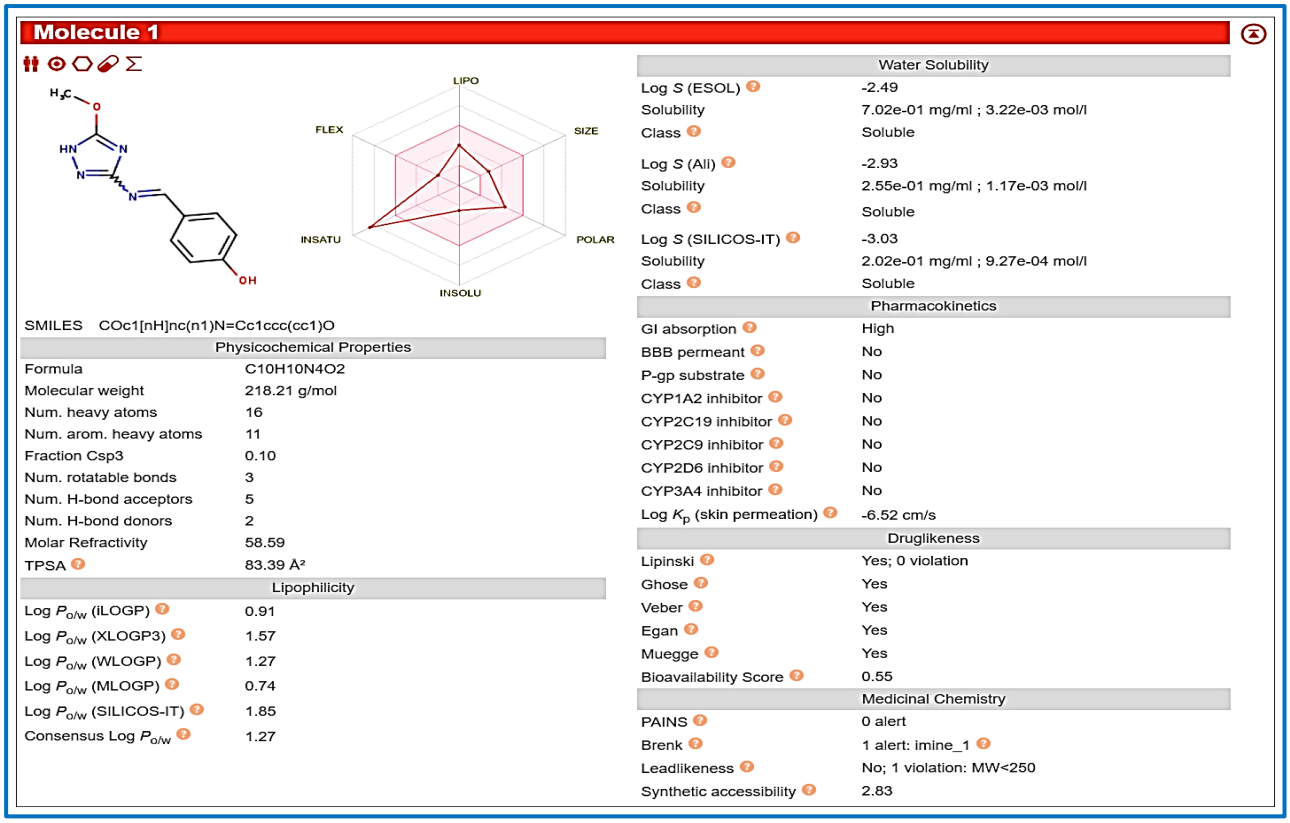

Molecule 1

SMILES COc1[nH]nc(n1)N=Cc1ccc(cc1)O

Physicochemical Properties	
Formula	C10H10N4O2
Molecular weight	218.21 g/mol
Num. heavy atoms	16
Num. arom. heavy atoms	11
Fraction Csp3	0.10
Num. rotatable bonds	3
Num. H-bond acceptors	5
Num. H-bond donors	2
Molar Refractivity	58.59
TPSA	83.39 Å²
Lipophilicity	
Log $P_{o/w}$ (iLOGP)	0.91
Log $P_{o/w}$ (XLOGP3)	1.57
Log $P_{o/w}$ (WLOGP)	1.27
Log $P_{o/w}$ (MLOGP)	0.74
Log $P_{o/w}$ (SILICOS-IT)	1.85
Consensus Log $P_{o/w}$	1.27

Water Solubility	
Log *S* (ESOL)	-2.49
Solubility	7.02e-01 mg/ml ; 3.22e-03 mol/l
Class	Soluble
Log *S* (Ali)	-2.93
Solubility	2.55e-01 mg/ml ; 1.17e-03 mol/l
Class	Soluble
Log *S* (SILICOS-IT)	-3.03
Solubility	2.02e-01 mg/ml ; 9.27e-04 mol/l
Class	Soluble
Pharmacokinetics	
GI absorption	High
BBB permeant	No
P-gp substrate	No
CYP1A2 inhibitor	No
CYP2C19 inhibitor	No
CYP2C9 inhibitor	No
CYP2D6 inhibitor	No
CYP3A4 inhibitor	No
Log K_p (skin permeation)	-6.52 cm/s
Druglikeness	
Lipinski	Yes; 0 violation
Ghose	Yes
Veber	Yes
Egan	Yes
Muegge	Yes
Bioavailability Score	0.55
Medicinal Chemistry	
PAINS	0 alert
Brenk	1 alert: imine_1
Leadlikeness	No; 1 violation: MW<250
Synthetic accessibility	2.83

Figure 18: SwissADME Prediction for derivative C.

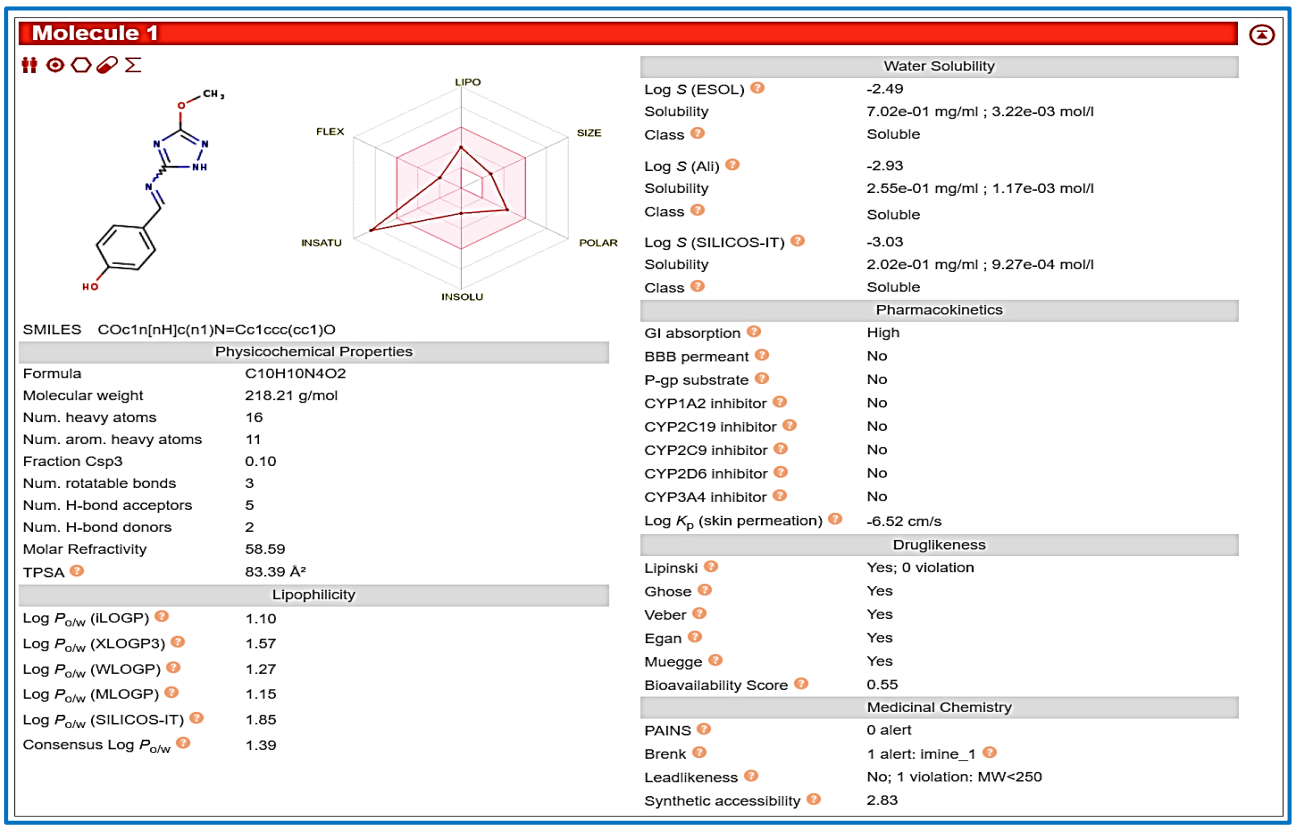

Molecule 1

SMILES COc1n[nH]c(n1)N=Cc1ccc(cc1)O

Physicochemical Properties	
Formula	C10H10N4O2
Molecular weight	218.21 g/mol
Num. heavy atoms	16
Num. arom. heavy atoms	11
Fraction Csp3	0.10
Num. rotatable bonds	3
Num. H-bond acceptors	5
Num. H-bond donors	2
Molar Refractivity	58.59
TPSA	83.39 Å²
Lipophilicity	
Log $P_{o/w}$ (iLOGP)	1.10
Log $P_{o/w}$ (XLOGP3)	1.57
Log $P_{o/w}$ (WLOGP)	1.27
Log $P_{o/w}$ (MLOGP)	1.15
Log $P_{o/w}$ (SILICOS-IT)	1.85
Consensus Log $P_{o/w}$	1.39

Water Solubility	
Log *S* (ESOL)	-2.49
Solubility	7.02e-01 mg/ml ; 3.22e-03 mol/l
Class	Soluble
Log *S* (Ali)	-2.93
Solubility	2.55e-01 mg/ml ; 1.17e-03 mol/l
Class	Soluble
Log *S* (SILICOS-IT)	-3.03
Solubility	2.02e-01 mg/ml ; 9.27e-04 mol/l
Class	Soluble
Pharmacokinetics	
GI absorption	High
BBB permeant	No
P-gp substrate	No
CYP1A2 inhibitor	No
CYP2C19 inhibitor	No
CYP2C9 inhibitor	No
CYP2D6 inhibitor	No
CYP3A4 inhibitor	No
Log K_p (skin permeation)	-6.52 cm/s
Druglikeness	
Lipinski	Yes; 0 violation
Ghose	Yes
Veber	Yes
Egan	Yes
Muegge	Yes
Bioavailability Score	0.55
Medicinal Chemistry	
PAINS	0 alert
Brenk	1 alert: imine_1
Leadlikeness	No; 1 violation: MW<250
Synthetic accessibility	2.83

Figure 19: SwissADME Prediction for derivative D.

4. Conclusion

This study shows that triazole–imine derivatives are versatile and physiologically active heterocyclic compounds. Successful synthesis and spectroscopic analysis demonstrate moderate structural modification of triazole-based Schiff bases. Thus, substituent type and concentration considerably alter antibacterial and cytotoxic properties, as compound C suppresses bacteria better while compound A kills PC-3 and MCF-7 cells. Molecular docking studies show that ligand-protein interactions in the 8RZX binding pocket survive via hydrogen bonding and π–π stacking. These data suggest electrical dispersion and aromaticity affect biological performance. Although promising, the study requires in vivo confirmation and selectivity testing against normal cells. The next research will focus on biological applications such antifungal screening, mechanistic apoptosis, and in vivo anticancer testing. Molecular dynamics simulations are essential to study ligand stability over time. Expanding the compound library and relating physicochemical aspects to biology may enhance structure–activity connections. This research provides a solid experimental and theoretical foundation for rationally constructing triazole–imine-based therapies.

5. References

[1] Kabir E, & Uzzaman, M. A review on biological and medicinal impact of heterocyclic compounds. 2022.

[2] Salah ARM. Heterocyclic Compounds in Modern Drug Design: Synthetic Strategies and Biological Targets. 2025.

[3] Nishanth Rao R, Jena S, Mukherjee M, Maiti B, Chanda K. Green synthesis of biologically active heterocycles of medicinal importance: A review. Environmental Chemistry Letters. 2021;19(4):3315–58.

[4] Jiali M, Chenghe Z, Xue B. Advances in triazole antimicrobial agents. 2010.

[5] -H. Zhou C, Wang Y. Recent researches in triazole compounds as medicinal drugs. Current medicinal chemistry. 2012;19(2):239–80.

[6] Bezerra Morais PA, Javarini CL, Valim TC, Francisco CS, de Freitas Ferreira LC, Trancoso Bottocim RR, et al. Triazole: a new perspective in medicinal chemistry and material science. Current Organic Chemistry. 2022;26(18):1691–702.

[7] Al Khulaifi RS, AlShehri MM, Al-Qadsy I, Al Jufareen MA, Saeed WS, Badjah-Hadj-Ahmed AY, et al. Breaking the Equilibrium and Improving the Yield of Schiff Base Reactions by Pervaporation: Application to a Reaction Involving n-butylamine and Benzaldehyde. Separations. 2023;10(12):602.

[8] Qian C, Feng L, Teo WL, Liu J, Zhou W, Wang D, et al. Imine and imine-derived linkages in two-dimensional covalent organic frameworks. Nature Reviews Chemistry. 2022;6(12):881–98.

[9] Qadir T, Amin A, Sharma PK, Jeelani I, Abe H. A review on medicinally important heterocyclic compounds. The Open Medicinal Chemistry Journal. 2022;16(1).

[10] Jaafar MR, Rasool BS, Jawad AA, Abbas AK, Hamid DM, Al-Tabra RH. Synthesis and Biological Activity of a Novel Derivatives of Schiff Base. Al-Nahrain Journal of Science. 2024;27(5):1–9.

[11] Beebany S, Jasim SS, Al-Tufah MM, Arslan S. Preparation and identification of new 1, 4-bis (5, 3-substituted-2, 3-dihydro-1H-pyrazole-1-yl) Buta-1, 4-Dione derivatives with their antibacterial effect evaluation. Chemical Methodologies. 2023;7:123–36.

[12] Eneama WA, Salman HH. Isoxazolidine Derivatives Exhibit Selective Antitumor Activity Against Breast Cancer Cells: Turunan Isoxazolidine Menunjukkan Aktivitas Antitumor Selektif Terhadap Sel Kanker Payudara. Academia Open. 2024;9(2):10.21070/acopen. 9.2024. 8148–10./acopen. 9.2024. 8148.

[13] Chatterjee O, Jana J, Panda S, Dutta A, Sharma A, Saurav S, et al. Remodeling Ca2+ dynamics by targeting a promising E-box containing G-quadruplex at ORAI1 promoter in triple-negative breast cancer. Cell calcium. 2024;123:102944.

[14] Zhong HA, Almahmoud S. Docking and selectivity studies of covalently bound Janus kinase 3 inhibitors. International Journal of Molecular Sciences. 2023;24(7):6023.

[15] Wajid M, Uzair M, Muhammad G, Siddique F, Ashraf A, Ahmad S, et al. Biological activities, DFT and molecular Docking studies of novel schiff bases derived from Sulfamethoxypyridazine. ChemistrySelect. 2024;9(15):e202400675.

[16] Walid A, Soeparman S, Wahyudi S, Sasongko MN, editors. Simulation of molecular dynamic between nickel oxide and water to improve water splitting performance by increasing energy kinetic and potential of water. THE 4TH INTERNATIONAL CONFERENCE ON SCIENCE AND TECHNOLOGY (ICST) 2021: Science for Excellence Development of Local Resources; 2023: AIP Publishing LLC.

[17] Prasanti M, Jha A, Kumar BR, Ch RK. Structural Aspects and Characterization of Synthesized Novel Schiff Base of 4-Hydroxybenzaldehyde with Anilines for Optoelectronic Properties. 2023.

[18] Khalaf MZ. Research Entitled (Spectroscopic And Thermodynamic Study Of A Number Of Charge Transfer Complexes Derived From The Reaction Of 3-Methoxy-4-

Hydroxybenzaldehyde And A Number Of Aromatic Amines With A Number Of Electronic Receptors. Central Asian Journal of Medical and Natural Science. 2024;5(4):539–48.

[19] Al-Tufah MM. Synthesis and Identification of Some New bi-azetidine 2, 2′-dione and bi-quinazoline-4, 4 ′-dione Compounds derived from bis Schiff Base derivatives. Samarra Journal of Pure and Applied Science. 2025;7(2):56–76.

[20] Kumar M, Singh AK, Singh AK, Yadav RK, Singh S, Singh AP, et al. Recent advances in 3d-block metal complexes with bi, tri, and tetradentate Schiff base ligands derived from salicylaldehyde and its derivatives: Synthesis, characterization and applications. Coordination Chemistry Reviews. 2023;488:215176.

[21] Abbas AK, Jber NR. Synthesis and characterization of new oxazepine compounds and estimation its biological activity. Al-Nahrain Journal of Science. 2020;23(3):17–23.

[22] Gul S, Jan F, Alam A, Shakoor A, Khan A, AlAsmari AF, et al. Synthesis, molecular docking and DFT analysis of novel bis-Schiff base derivatives with thiobarbituric acid for α-glucosidase inhibition assessment. Scientific Reports. 2024;14(1):3419.

[23] Hamed AA, Ali EA, Abdelhamid IA, Saad GR, Elsabee MZ. Synthesis of novel chitosan-Schiff bases nanoparticles for high efficiency Helicobacter pylori inhibition. International Journal of Biological Macromolecules. 2024;274:133499.

[24] Al-Badrany K, Jasim S, Al-Tufah M. Synthesis of some of the compounds of Chalcones and pyrozoline containing phthalimide unit and evaluation their biological activity of some of them. Samarra Journal of Pure and Applied Science. 2020;2(4).

[25] Alamri AA, Borik RM, El-Wahab AHA, Mohamed HM, Ismail KS, El-Aassar MR, et al. Synthesis of Schiff bases based on Chitosan, thermal stability and evaluation of antimicrobial and antitumor activities. Scientific Reports. 2025;15(1):892.

[26] La Serra MA. Exploring RHOGTPases: a computational study of protein-protein interactions and drug design. 2024.